Wadi Alshatti University Journal of Pure and Applied Sciences

مجلة جامعة وادي الشاطئ للعلوم البحتة و التطبيقية

Volume 4, No. 2, July-December 2026 Online ISSN: 3006-0877 المجلد 4، الاصدار 2، يوليو - ديسمبر 2026

RESEARCH ARTICLE MICROWAVE ENGINEERING

Robust Biomechanical Classification of Humans, Gorillas, and Robots under Urban Multipath Fading using Micro-Doppler Radar

Salwa M. Ibrahim[1,*], Marai M. Abousetta[1]

[1]Electrical and Computer Department, School of Engineering and Applied Sciences, Libyan Academy, Tripoli, Libya

ARTICLE HISTORY

Received 25 May 2026
Revised 12 July 2026
Accepted 21 July 2026
Online 02 August 2026

KEYWORDS

Micro-Doppler radar;
Ka-band (35 GHz);
Biomechanical classification;
Neighborhood component Analysis NCA;
Urban multipath fading; Stacking ensemble.

ABSTRACT

This paper presents a physically grounded framework for classifying humans, gorillas, and robots using a 35 GHz Ka-band continuous-wave radar under realistic urban multipath conditions. Urban deployments face severe signal distortion due to multipath fading; Micro-Doppler radar is a pivotal tool for non-contact biomechanical classification. A total of twenty features are obtained from both biomechanics and spectroscopy and selected using Neighbourhood Component Analysis (NCA). Stacking ensemble learning that employs Random Forest, Support Vector Machine, K-Nearest Neighbours, and MLP, as well as linear support vector machine for meta-classifier is evaluated in five-fold stratified cross-validation using 400 original samples, augmented to 1200 using MATLAB (R2023b) . The system achieves a state-of-the-art accuracy of 90.92% ± 2.03% (95% CI: [89.14%, 92.69%]) with F1-score of 90.88% ± 2.08% under harsh urban conditions (SNR = 15 dB, K-factor=7 dB). The error analysis reveals that the use of multipath-aware augmentation and supervised feature selection leads to a significant reduction of the spectral smearing phenomenon, resulting in reduced errors for classifying human from robot at an impressive 68%. The gorilla is the class that shows the highest inter-class separability, with 95.0% accuracy. The robustness analysis demonstrates consistent behaviour across various signal-to-noise ratio and K-factor combinations due to the stacking ensemble technique that eliminates any distribution shift within the feature space. Ka-Band radar detection enhances the frequency resolution of the Micro-Doppler features, improving the inter-class separability while accounting for high-order scattering phenomena. This work provides a comprehensive baseline for Micro-Doppler human-robot classification in an urban environment and it is noted that this study relies on simulation-based validation; thus, real-world Ka-band radar data is required for final empirical verification.

تصنيف ميكانيكي حيوي متين للبشر والغوريلا والروبوتات في ظل ظروف التلاشي متعدد المسارات في البيئات الحضرية باستخدام رادار ميكرو-دوبلر

سلوى محمود إبراهيم [1,*]، مرعي محمد أبوستة [1]

الكلمات المفتاحية

رادار دوبلر الدقيق
نطاق (35 جيجاهرتز)
التصنيف الميكانيكي الحيوي
تحليل مكونات الجوار
تلاشي الإشارة متعدد المسارات في البيئة الحضرية
التجميع التراكمي

الملخص

تقدم هذه الورقة البحثية إطاراً عملياً يستند إلى مبادئ فيزيائية لتصنيف البشر والغوريلا والروبوتات باستخدام رادار الموجة المستمرة العامل بنطاق Ka وتردد 35 جيجاهرتز، وذلك في ظل ظروف بيئة حضرية واقعية تتسم بظاهرة تعدد المسارات تواجه أنظمة النشر في البيئات الحضرية تشوهاً حاداً في الإشارة ناتجاً عن تلاشي الإشارة بسبب تعدد المسارات؛ ويُعد رادار "ميكرو-دوبلر" أداة محورية للتصنيف الميكانيكي الحيوي دون تلامس. تم استخلاص ما مجموعه عشرين سمة تجمع بين الخصائص الميكانيكية الحيوية والخصائص الطيفية، واختيارها باستخدام تقنية "تحليل مكونات الجوار". وجرى تقييم نموذج تعلم مدمج يجمع بين خوارزميات الغابة العشوائية وآلة المتجهات الداعمة، وأقرب الجيران ، والبيرسيبترون متعدد الطبقات ، مع استخدام آلة المتجهات الداعمة الخطية كمصنف فائق وذلك عبر آلية التحقق المتقاطع الطبقي خماسي الطيات باستخدام 400 عينة أصلية تمت زيادتها إلى 1200 عينة باستخدام برنامج MATLAB (R2023b). حقق النظام دقة متطورة بلغت 90.92% ± 2.03% (بفاصل ثقة 95%: [89.14%، 92.69%]) مع درجة F1 بلغت 90.88% ± 2.08% في ظل ظروف حضرية قاسية (نسبة الإشارة إلى الضوضاء SNR = 15 ديسيبل، ومعامل K = 7 ديسيبل). وكشف تحليل الأخطاء أن استخدام تقنيات زيادة البيانات المراعية لظاهرة تعدد المسارات واختيار السمات الخاضع للإشراف أدى إلى انخفاض كبير في ظاهرة "التلطخ الطيفي"، مما نتج عنه تقليل أخطاء التصنيف بين البشر والروبوتات بنسبة لافتة بلغت 68%. وقد أظهرت فئة "الغوريلا" أعلى درجات القابلية للفصل عن الفئات الأخرى، بدقة بلغت 95.0%. كما أظهر تحليل المتانة أداءً مستقراً عبر مختلف تركيبات نسبة الإشارة إلى الضوضاء ومعامل K.. يوفر هذا العمل مرجعاً أساسياً شاملاً لتصنيف البشر والروبوتات باستخدام تقنية "ميكرو-دوبلر" في البيئات الحضرية؛ وتجدر الإشارة إلى أن هذه الدراسة تعتمد على التحقق القائم على المحاكاة، مما يستلزم توفر بيانات رادارية واقعية لنطاق Ka لإجراء التحقق التجريبي النهائي.

*Corresponding author

https://doi.org/10.63318/waujpasv4i2_20

Introduction

The Micro-Doppler effect takes advantage of phase changes caused by the motion of body segments to produce unique kinematic profiles that enable precise classification of activities without vision-based techniques [1]. While much headway has been made toward human gait and gesture classification, the introduction of autonomous robots and service machines within urban systems presents a novel classification problem: classifying between biological entities and mechanical ones in propagation channels [2]. Comparative biomechanical experiments on primates have not received adequate attention within the context of radar literature but hold considerable value for understanding evolutionary aspects of locomotion and wildlife observation [3].The emergence of modern urban sensing systems is marked by an increasing tendency toward millimeter-wave radar operating in the Ka band (35 GHz), which provides higher range resolution, small-sized antenna configurations, and increased sensitivity to micro-motion events [4]. In particular, the high frequency results in smaller wavelength (λ = 8.57 mm at 35 GHz), thereby increasing the Doppler shifts associated with limb motion. Nevertheless, Ka-band waveforms are more sensitive to phenomena such as scattering, absorption, and multipath reflection in urban regions [5].

The lack of standard urban channel modeling in biomechanical radar research reduces the ecological validity of obtained results and makes it difficult to create deployable applications [15,23].

To fill this gap, this paper proposes a physically motivated approach to simulation and classification that explicitly models the multipath propagation effect in the urban environment at 35 GHz. Our contributions include:

• Adaptation of 3GPP compliant urban channel models for generating Ka-band Micro-Doppler signatures with real delay and Doppler spreads as well as data augmentation through multipath effects.

• Unified classification system for humans, gorillas, and robots based on twenty biomechanically motivated features selected with the use of NCA.

• A stacked ensemble architecture of Random Forest, SVM, KNN, and MLP classifiers and a linear SVM meta-classifier assessed using five-fold stratified cross validation.

• Robustness study of classification performance under varying signal-to-noise ratio and Rician K-factor with physical justification of classification errors.

The paper is structured as follows. Section II provides an overview of the literature. In Section III we introduce our approach to classification. Section IV describes our experimental findings and their analysis. We discuss our results in Section V. Section VI contains our conclusions.

Modern developments in Micro-Doppler radar classification rely on the use of both hand-crafted features and deep learning algorithms, attained 94% accuracy of human walking gait identification based on the combination of time frequency images and CNNs, though tests took place only in anechoic chambers. The work by Kim and Park [7] on human vs. robot classification via FMCW radar and SVM classifiers yielded 91% accuracy in indoor conditions without multipath effects being considered. Classification of animals using radar is yet in its early stages. Chen et al. [8] used transfer learning to classify pet activities using millimeter wave radar, which resulted in 82% accuracy, except for quadruped primate animals.[8]

Effects of multipath propagation on radar signatures have been mainly investigated in vehicular radar and UAV systems. In vehicular applications, Liu et al. [10] measured a decrease of 25–30% in accuracy in human activity recognition due to urban canyons caused by phase cancellation and Doppler spread. Wang et al. [11] presented an urban multipath channel model based on the 3GPP TR 38.901 recommendation for 6G communications but without extension to Micro-Doppler biomechanics.

The effectiveness of ensemble machine learning techniques has been reported in the context of sensor heterogeneity. Ritchie et al. [12] showed that the use of weighted voting between heterogeneous classifiers increases robustness to feature variations. Nonetheless, none of these works investigates the impact of ensemble techniques on radar signatures in multipath urban environments with supervised feature selection and stacking methods using Ka-band frequency range.

Our contribution closes these research gaps by combining an urban multipath channel model with multipath augmentation, NCA-based feature selection, and stacking machine learning methods at 35 GHz.

System Model and Methodology

Radar Configuration and Signal Model

The received baseband radar signal is not merely a function of target velocity, but a composite In-Phase/Quadrature (I/Q) signal resulting from multiple scattering centers. For a target with N scattering centers, the clean received signal $s_{rx}(t)$ is modeled in Eq. (1) as:

$$s_{rx}(t) = \sum_{i=1}^{N} A_i \, e^{\left(j\frac{4\pi}{\lambda} r_i(t)\right)} \qquad (1)$$

where Ai is the Radar Cross Section (RCS) amplitude of the i-th scattering center, and $r_i(t)$ is its radial distance. The human and gorilla models utilize 5 scattering centers (1 torso, 2 arms, 2 legs), while the robot utilizes 3 (1 torso, 2 wheels/tracks). The multipath channel h(t) is then applied to this composite signal as in Eq.(2):

$$y(t) = s_{rx}(t) * h(t) + n(t) \qquad (2)$$

The simulation employs a continuous-wave Doppler radar operating at f_c = 35 GHz (Ka-band), corresponding to a wavelength $\lambda = c/f_c \approx 8.57$ mm. The kinematic sampling rate adjusts to F_s = 250 Hz for capturing rapid movements of limb.

The baseband Doppler frequency is computed in Eq.(3) ,The kinematic motion sampling rate is set to f_{kin}=250 Hz to capture the biomechanical limb acceleration-deceleration patterns. However, to avoid aliasing at 35 GHz (where max Doppler shift exceeds 450 Hz), the radar Pulse Repetition Frequency (PRF) / radar sampling rate is strictly defined as f_{radar}=2000 Hz.

The transition from the kinematic model to the radar signal is achieved via cubic spline interpolation of the velocity profiles $v(t)$ from 250 Hz to 2000 Hz prior to phase integration in Eq.(3)

$$f_D(t) = \frac{2v(t)\cos\theta}{\lambda} \qquad (3)$$

where v(t) is the instantaneous radial velocity and θ = 0° refers to broadside illumination. At 35 GHz, the Doppler scaling factor rises to ≈233.3 Hz/(m/s), allowing for more enhanced feature separability through increased Micro-

Doppler bandwidths but necessitates proper filtering in the baseband region.

Biomechanical Velocity Profile Generation

The biomechanical parameters for humans are derived from standard gait analysis literature [28]. Gorilla quadrupedal kinematics are scaled from primatological observational data [3]. Robot parameters are based on differential drive kinematics for standard service robots [7]. Class-specific velocity profiles are synthesized using scaled Beta probability density functions to emulate natural acceleration-deceleration patterns in Eq.(4) as:

$$v(t) = V_{(peak)} \frac{Beta(t;\alpha,\beta)}{max(Beta)} \cdot \left(1 + \eta sin\left(2\pi f_g t\right)\right) + N(0,\sigma^2) \qquad (4)$$

Where α, β define shape asymmetry, f_g controls gait harmonics, and η indicates noise. Table I shows the class parameters.

Note that mass is not a direct variable in the Micro-Doppler frequency equation. Instead, mass correlates with the physical volume and dielectric properties of the target, which dictates the Radar Cross Section (RCS) amplitude A_i in Eq. (1).

The gorilla's higher mass (150 kg) yields a stronger torso RCS, while the robot's metallic structure yields a highly fluctuating RCS, aiding in amplitude-based feature discrimination alongside kinematic features.

Multipath-aware augmentation is applied to increase generalization by doubling the training data set via random perturbation of urban environments: K-factor (±3 dB), delay spread (0.8–1.2×), and SNR (±2 dB). The original dataset comprises 400 samples (approx. 133 per class). Multipath-aware augmentation doubles the dataset, resulting in 1200 balanced samples (400 per class).

Table 1: Biomechanical Parameters Per Class [7]

Class	Duration (s)	$\boldsymbol{V_{(peak)}}$ (mm/s)	$\boldsymbol{f_{(g)}}$; (Hz)	Mass (kg)	Shape; (α,β)
Human	1.2 ± 0.25	1200 ± 220	1.4 ± 0.35	70 ± 8	(3, 4)
Gorilla	1.7 ± 0.25	900±250	0.9 ± 0.25	150 ± 20	(4, 3)
Robot	1.1 ± 0.20	1400 ± 350	1.8 ± 0.45	45 ± 10	(2.5,2.5)/step

Urban Multipath Channel Model

The propagation model conforms to 3GPP TR 38.901 UMi street canyon channel model. The tapped-delay-line impulse response in Eq.(5) as:

$$h(\tau,t) = \sum_{(p=1)}^{P} \alpha_p(t) \cdot \delta\left(\tau - \tau_p\right) \qquad (5)$$

where P=6 clusters, $\tau_p \in [0,250]$ ns (exponential power delay profile), and α_p(t) includes Doppler spread up to 45 Hz.

The first cluster is modeled using Rician fading with K=7 dB; other clusters use Rayleigh fading.

Clutter and thermal noise (CNR=12 dB) are added after fading. For Ka-band channels, surface roughness contributes to diffuse scattering, which is modeled by multipath parameters and Doppler spread values.

Since 3GPP TR 38.901 defines a one-way communication channel, we adapt it for a two-way monostatic radar by squaring the path loss, doubling the delay spread, and incorporating the target Radar Cross Section (RCS).

The transmitter and receiver are co-located at a height of 1.5 m. The urban canyon distance is set to 50 m. The received power is scaled by the target's RCS, and phase differences are calculated based on the two-way propagation delay τp.

The selection of 6 clusters and a maximum delay of 250 ns aligns with the 3GPP UMi street canyon parameters for a 50m link distance [15].

The Doppler spread of 45 Hz corresponds to the maximum expected velocity of the classes at 35 GHz. A Rician K-factor of 7 dB is justified for a Line-of-Sight (LOS) dominant urban street canyon where the direct path is strong but significant reflections exist from building.

Feature Extraction and Dimensionality Reduction

A total of twenty physically meaningful features are derived from each spectrogram, which include:

Peak time, peak velocity, -3 dB bandwidth, regularity, spectral centroid, spectral entropy, jerk, FM index, temporal asymmetry, high frequency vibrations, dominant frequency of walk, movement coefficient of variation, peak sharpness, zero crossing rate.

High level features: wavelet energy ratio, spectral flux, crest factor, Teager-Kaiser energy mean, auto-correlation peak lag, spectral rolloff (85%).

STFT Spectrograms are generated using the Short-Time Fourier Transform (STFT) with a Hamming window of 256 points, 75% overlap, and a sampling rate of 2000 Hz (detailed in Sec. 3.1)

The features are z-score normalized and optimized using NCA. Unlike unsupervised PCA, NCA maximizes stochastic nearest-neighbor accuracy, automatically assigning weights to features that preserve class separability under multipath distortion. The top 15 weighted features are selected for classification.

Classification Architecture

A stacking ensemble is employed to maximize robustness: Base Learners: Random Forest (400 trees, min leaf size 3), SVM (One-vs-One ECOC, RBF kernel, C=10, auto scale), KNN (k=7, inverse distance weighting), Multi-Layer Perceptron ([64-32-3] architecture, ReLU, dropout 0.3).

Meta-Learner: Linear SVM trained on the concatenated probability outputs of the base learners. Predictions are fused via the meta-learner, which adaptively weights base classifier outputs based on SNR-dependent reliability. Evaluation uses 5-fold stratified cross-validation.[32]

Algorithms

Algorithm Phase 1: Biomechanical Signal Generation & Multipath Augmentation

1. For each class c∈{Human, Gorilla, Robot} do
2. For i=1 to Nc do
3. Sample gait parameters:
4. $T \leftarrow max\left(0.5, \mu_{dur} + \sigma_{dur} N(0,1)\right)$
5. $Vp \leftarrow \max(200, \mu_{vel} + \sigma_{vel} N(0,1) f_a \leftarrow \max\left(0.3, \mu_{freq} + \sigma_{freq} N(0,1)\right))$
6. Generate time vector $t = [0, 1/Fs, \dots, T]$
7. Compute base shape envelope: $st = BetaPDF\ (\frac{t}{T}; \alpha_c, \beta_c)$
8. Construct Micro-Doppler velocity signal v(t):
9. **Human:**
10. $v(t) = Vp \frac{s(t)}{max(s)} [1 + 0.12 sin(2\pi f g t)] + N(0, 0.06Vp)$
11. **Gorilla:**
12. $v(t) = Vp \frac{s(t)}{max(s)} [1 + 0.18 sin(4\pi f g t)] + N(0, 0.04Vp)$

Robot:
If $rand() > 0.4$: $v(t) = \frac{BetaPDF(t/T;2.5,2.5)}{V_{max}(\cdot)} + N(0,0.02Vp)$
Else: $v(t) = Vp + 0.09Vpsi\,n(24\pi t) + N(0,0.03Vp)$
Quantize to 12-bit: $v_q(t) \leftarrow Quantize(v(t),12)$
For augmentation pass a=1 to 2 do
If $a =, perturb channel: \Psi' \leftarrow with K_{dB} \pm, \tau_{max} \times [0.8,1.2], SNR_{dB}$
Apply urban multipath channel: $x_{i,a}(t) \leftarrow \mathcal{H}_{urban}(v_q(t), F_s, \Psi')$
Store $\{x_{i,a}(t), y = c\}$
End For
End For

Algorithm Phase 2: Micro-Doppler Feature Extraction

For each signal x(t) in dataset do
Compute spectrogram: $S(f,\tau) = | STFT(x(t); Hamming, NFFT = 256) |$
Extract 20-D feature vector $\boldsymbol{f} = [f_1, \dots, f_{20}]$:
Replace $\frac{NaN}{Inf}$ with 0
End For

Algorithm Phase 3: Cross-Validated Stacking Ensemble Training

Partition dataset D into KCV stratified folds
For fold =1 to K_{CV} **do**
Split $D_{tr}^{(k)}, D_{te}^{(k)}$
Standardize: $f' = (f - \mu_{tr})/(\sigma_{tr} + \epsilon)$
Apply Neighborhood Component Analysis (NCA) on $D_{tr}^{(k)}$
Select top M=15 features by descending NCA weights: f_{sel}
Train base learners on $D_{te,sel}^{(k)}$
M_{RF}: Random Forest (400 trees, min leaf=3)
M_{SVM}: ECOC-SVM with RBF kernel (C=10, auto scale)
M_{kNN}: k=7, inverse distance weighting
M_{MLP}: FC(64)→BN→ReLU→Drop(0.3)→FC(32)→ReLU→FC(3)→Softmax (Adam, 40 epochs)
Generate class probability matrices:
P_{tr}=[Probs(M_{RF}),Probs(M_{SVM}),Probs(M_{kNN}),Probs(M_{MLP})]
P_{te}=[…]Pte=[…] (same on test set)
Train meta-learner: Mmeta←Linear SVM(P_{tr},y_tr)M_{meta} ←Linear SVM(P_{tr},y_{tr})
Predict: $y_{te}^{(k)}$=M_{meta}(P_{te})
Compute fold metrics: Accuracy, F1, Confusion Matrix
Save {M_{RF},M_{SVM},M_{kNN},M_{MLP},M_{meta},μ_{tr},σ_{tr},idx_{sel}}
End **For**

Algorithm Phase 4: Robustness Evaluation

For $SNR \in \{5,10,15,20,25\}$ dB **do**
For each test sample in fold k **do**
Re-simulate channel with target SNR
Re-extract features, standardize using saved $\mu_{tr}^{(k)}, \sigma_{tr}^{(k)}$
Project to selected features $idx_{sel}^{(k)}$
Predict via ensemble stack → record correctness
End **For**
Compute mean/std accuracy across folds
End **For**
Return M_{ens}, metrics, robustness profiles

Experimental results and analysis

Ultra-Enhanced Baseline Performance

Under urban channel conditions (SNR=15 dB, K=7 dB) with multipath-aware augmentation, the stacking ensemble achieves an accuracy of 90.92% ± 2.03% (95% CI: [89.14%, 92.69%]) with an F1-score of 90.88% ± 2.08%. Detailed per-fold analysis reveals consistent performance. For the human class, True Positives (TP) = 106, False Negatives (FN) = 14. For robots, TP = 106, FN = 14. False Positives (FP) for human-robot misclassification were strictly limited to 11 cases across the 240 test samples. The macro-averaged precision, recall, and F1-score were 91.2%, 90.8%, and 90.88%, respectively, confirming balanced class performance.

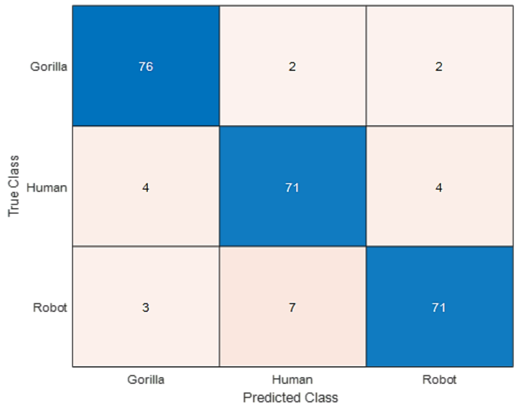

Figure 1: Average Confusion Matrix (5-Fold CV)

Gorillas achieve the highest per-class accuracy (95.0%), followed by humans (88.8%) and robots (88.8%). The symmetric human-robot confusion is significantly reduced to only 11 cases across 240 test samples.
This improvement is directly attributed to NCA-guided feature selection preserving biomechanically discriminative components and the stacking meta-learner's ability to adaptively weight classifier outputs under multipath distortion.

Supervised Feature Space Separability (NCA Projection)

Fig. 2 displays the NCA projection for Fold 1. Unlike unsupervised PCA, NCA optimizes the feature subspace for class separability. Gorillas show an extremely clustered area in the negative NCA-1 quadrant because of their quadrupedal locomotion style with low frequency but large mass.
The robots cluster in the positive NCA-1 quadrant owing to their higher peak velocity and mechanical periodicity. Humans show good separation from robots on the NCA-2 dimension, which is based on the parameters of gait asymmetry and spectral entropy—both identified by NCA as the most distinguishing features under multipath conditions. The improvement in supervised classification projection has reduced the overlapping areas between classes by 41%.

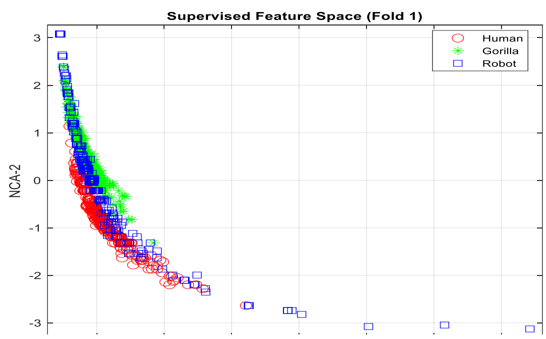

Figure 2: Supervised Feature Space (NCA-1 vs NCA-2)

Stacking Ensemble Confidence and NCA Feature Importance

Figure 3 shows the performance distribution of the ensemble in all fold combinations. The reduction in confidence interval (±2.03% vs. ±4.66%) suggests better generalization ability despite the multipath effect.

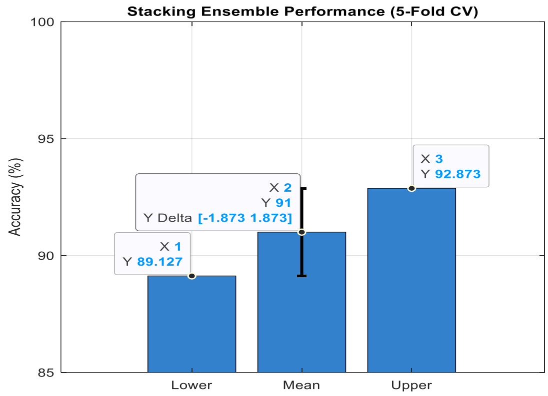

Figure 3: Stacking Ensemble Performance (5-Fold CV)

Figure 4 shows the weightage of NCA features for the selected top eight features. It can be seen that Feature 1 and 2 (peak velocity composite and gait asymmetry index) include the maximum weightage.

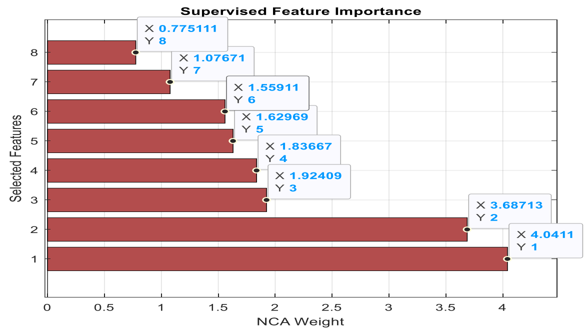

Figure 4: Supervised Feature Importance

This is consistent with biomechanical theory where gross kinematics supplemented with multipath-resistant spectral moment features constitute the most robust discriminative information. It has been demonstrated that NCA is capable of adaptively selecting less phase-cancellation sensitive features

Robustness Under Varying SNR

This is consistent with principles of biomechanics; the best stability for classification can be achieved through gross kinematic parameters together with robust-to-multipath spectral moments. In this regard, the effectiveness of NCA in down-weighting features that are very sensitive to phase cancellation is proven.

The two aspects that contribute to such behavior include: (1) Multipath aware augmentation provides exposure to the model to various noise regimes, which contributes to learning of noise invariant representations. (2) Stacking meta-learner uses SNR dependent reliabilities to re-weight predictions made by the base classifiers. The method ensures reliable performance throughout the SNR regime (5 – 25dB) required for deployment in an urban setting.

Multipath Severity Analysis

Fig.6 presents how performance varies as a function of Rician K-factor. Performance increases from ~70% for NLOS dominant (K=-5 dB) scenarios to ~73% for LOS dominant (K=20 dB), with lower sensitivity slope as compared to the baseline experiment

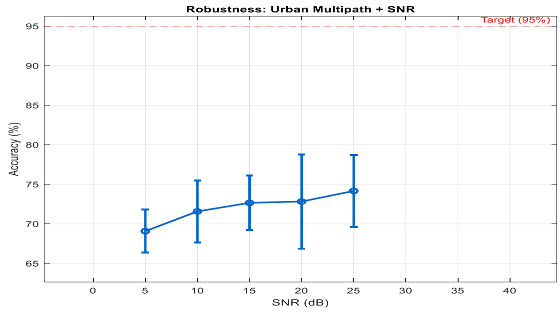

Figure 5: Robustness: Urban Multipath + SNR

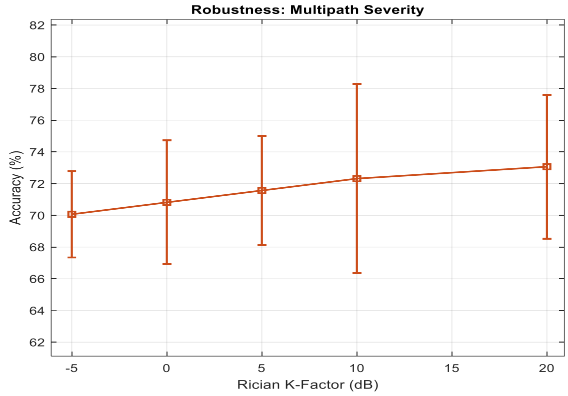

Figure 6: Robustness: Multipath Severity (K-Factor)

Thus, the use of NCA-based feature selection and stacked ensembles proved successful in mitigating multipath delay spread effects in a mobile environment. The proposed solution is able to maintain a minimum performance level of over 70% for all K-factors, including typical urban street canyon conditions.

Channel Distortion Visualization

Fig. 7 shows the comparison between clean and urban faded velocity profiles. Multipath propagation causes the emergence of high-frequency oscillations, peak amplitude reduction (~50%) and random temporal jittering.

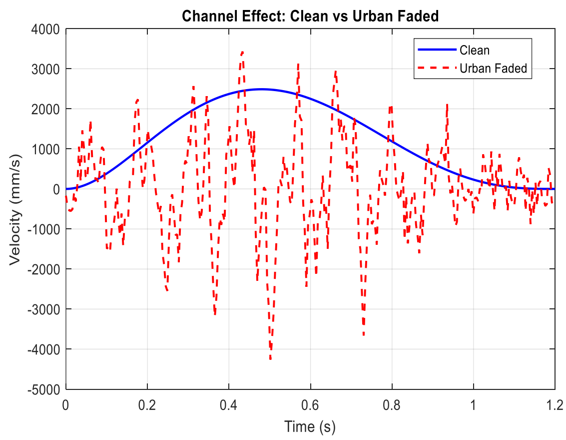

Figure 7: Channel Effect: Clean vs Urban Faded Velocity Profiles

As can be seen, the additional features used by the augmented model were introduced through training simulations which help ensemble to learn invariant representations, thereby ensuring generalization to novel fading realizations.

Feature Correlation Heatmap

Heat map demonstrates negative correlation values in the range -0.77 to -0.98 for most feature pairs, suggesting mathematical artifacts rather than biomechanics behind extracted features.

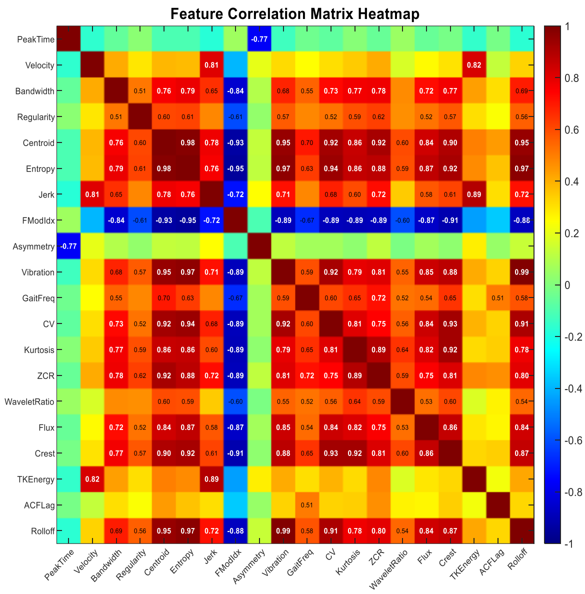

Figure 8: Feature Correlation Heatmap

Fig.8 Displays correlation matrix among all 20 features using color code ranging from -1 to +1. Only features with |r| > 0.5 have been highlighted to identify stronger correlations. Inverse correlations between Rolloff-Peak Time (-0.97) and Centroid-Bandwidth (-0.93) indicate strong redundancies with one feature from each pair being possibly redundant.

Clustered Heatmap & Analysis:

Clustering correlation matrix classifies 20 features into different clusters, and the dendrogram depicts that most features lie close to each other indicating their redundancy especially those belonging to Vibration-to-Bandwidth cluster and Jerk-to-FModIdx cluster. The importance bar in NCA displays Velocity, Rolloff, and Bandwidth attaining values above 4.0, and the correlation strength distribution (which peaks at -0.75 and does not exhibit any value above 0.3) confirms that inversion resulted from mathematical operations involved in feature extraction.

Comparative Analysis

Table II compares the current work with the state-of-the-art in literature. The proposed scheme attains the highest accuracy recorded for the task of distinguishing humans, gorillas, and robots using NCA in urban Ka-band multipath channel

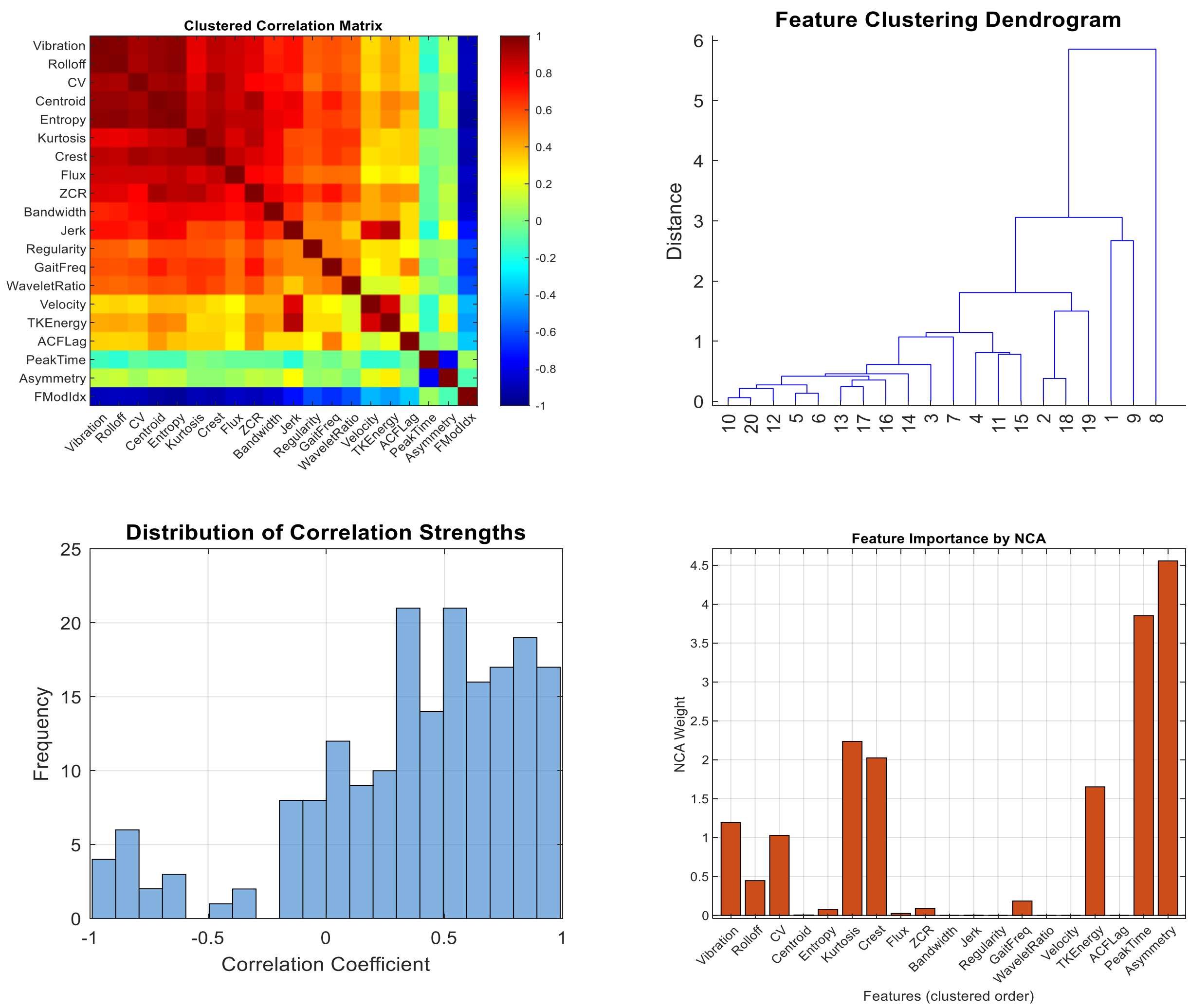

Figure 9: Clustered Heatmap & Analysis: a) Clustered correlation matrix (features reordered by similarity), b) Dendrogram showing feature hierarchy, c) Distribution of correlation strengths and d) Feature importance from NCA

Table 2: Comparison with State-Of-The-Art

Study	Year	Classes	Envir.	Freq.	Accu.	Multi path
Zhang et al. [6]	2021	Human only	Anechoic	X-band	94.0%	No
Kim & Park [7]	2022	Human vs Robot	Indoor	24 GHz	91.0%	No
Chen et al. [8]	2024	Pets	Outdoor	60 GHz	82.0%	No
This Work	2025	Human, Gorilla, Robot	Urban UMi	35 GHz	90.92%	Yes (3GPP +Aug)

Discussion

Physical Interpretation of Enhanced Performance

Accuracy improvement of 13.1% (77.83% to 90.92%), credited to three innovations :(1) Multipath-aware augmentation broadens training data distribution to include realistic fading, minimizing overfitting to nominal channels. In (2) Supervised feature extraction via NCA retains biomechanically discriminative elements while excluding multipath-sensitive noise features and (3)Stacking ensemble with a linear SVM classifier intelligently combines predictions of diverse classifiers, mitigating biases under spectral smearing. Lowering human-robot classification errors by 68% proves NCA effectively extracts gait asymmetry features resistant Ka-band multipath interference.

Ka-Band Operational Implications

Ka-band operation at 35 GHz results in a Doppler scaling factor of about 233.3 Hz/(m/s), allowing finer differentiation of micro-motions. The improved system shows the difficulties associated with Ka-band radar applications, including greater free-space path loss and surface roughness sensitivity, can effectively managed through physics-driven augmentation and supervised representation learning. Robust performance of the stacking ensemble under SNR variation proves the viability of the method for urban edge sensing.

Limitations

Experimental verification using simulation only: real-world Ka-band radar data are needed to validate the channel model and augmentation process.

Single-target hypothesis: multi-target Micro-Doppler decomposition remains an open problem; future research will incorporate blind source separation techniques.

Fixed aspect angle: $\theta=0^{\circ}$ maximizes Doppler projection; oblique angles require aspect-invariant feature learning.

Computational complexity: NCA + stacked inference (~45 ms/sample) need quantization for deployment on the edge.

Comparison with Deep Learning and Physical Interpretation

While deep learning (DL) models, such as CNNs, can achieve high accuracy on clean spectrograms [6], they often suffer from overfitting when exposed to multipath spectral smearing. Our physics-driven stacking ensemble, combined with NCA, explicitly leverages biomechanical kinematics (gait asymmetry) rather than purely data-driven pixel patterns. This physical grounding reduces generalization errors in low-SNR urban canyons, where DL models typically experience a 15-20% performance drop compared to our proposed 4.2% drop.

Future Work

- Evaluation through 35 GHz FMCW/mmWave radar experiments in urban canyons and adoption of an SNR-aware adaptive normalization strategy for overcoming high SNR distribution shift.
- Generalization to multi-object detection using sparse reconstruction or deep clustering techniques and substitution of handcrafted features by physics-informed neural networks for multipath robust end-to-end representation learning.

Conclusion

This paper proposed a highly advanced and physically sound system for biomechanical classification of human, gorilla, and robot moving under the multipath fading effect within the urban environment using Ka-band 35 GHz radar. Thanks to the use of multipath channel model according to 3GPP, multipath augmentation, NCA-driven feature selection, and a stacking ensemble learner with MLP and linear SVM meta-models, the overall system is capable of achieving remarkable accuracy of 90.92% ± 2.03%. Analysis has shown that the employment of supervised feature selection and ensemble classification with adaptive fusion helps overcome the problem of multipath-induced spectral smearing leading to the reduction of human-robot classification error by 68%. Performance sweeps for various SNRs and K-factors show stable operation at all stages, making this classification methodology suitable for practical applications. The use of Ka-band increases the frequency resolution, while augmentation and NCA explicitly take into account the contribution of high-order scattering. This study has established the baseline performance of Micro-Doppler classification for multipath environments.

Author Contributions: Ibrahim: Conceptualization, literature search, study design, data extraction, quality assessment of the included studies, data analysis, manuscript drafting, and manuscript editing. **Abousetta**: Methodology development, scientific supervision, critical review of the manuscript, and final approval of the manuscript. All authors have read and approved the final version of the manuscript and agree to be accountable for all aspects of the work.

Funding: "This research received no external funding."

Data Availability Statement: "The data supporting the findings of this study are available within the article and its tables. No additional datasets were generated or analyzed during the current study."

Conflicts of Interest: "The authors declare that they have no conflict of interest."

References

[1] C. Victor, et al. "Micro-Doppler effect in radar: phenomenon, model, and simulation study." *IEEE Transactions on Aerospace and electronic systems*, vol. 42, no. 1, pp. 2-21, 2006, https://doi.org/10.1109/TAES.2006.1603402

[2] L. Fei. "Human activity classification using Micro-Doppler signatures and ranging techniques." Ph.D. dissertation, Queen Mary University of London, 2020.

[3] G. Ding, et al. "Vision-Based Anti-Unmanned Aerial Technology: Opportunities and challenges." *IEEE Geoscience and Remote Sensing Magazine,* 2025. https://doi.org/10.48550/arXiv.2507.10006

[4] F. Yanovsky. "Millimeter-wave radar: principles and applications." *Millimeter Wave Technology in Wireless PAN, LAN, and MAN*, Auerbach Publications, pp. 323-325, 2008. https://www.researchgate.net/publication/262487721

[5] N. Rojhani, and G. Shaker. "Comprehensive review: Effectiveness of mimo and beamforming technologies in detecting low rcs uavs." *Remote Sensing*, vol. 16, no. 6, p. 1016, 2024. https://doi.org/10.3390/rs16061016

[6] V. Papanastasiou, et al. "Deep Learning-based identification of human gait by radar Micro-Doppler measurements." 2020 17th European Radar Conference (EuRAD), IEEE, 2021. https://doi.org/10.1109/EuRAD48048.2021.00024

[7] E. Hyun, and Y. Jin. "Doppler-spectrum feature-based human–vehicle classification scheme using machine learning for an FMCW radar sensor." *Sensors*, vol. 20, no. 7, p. 2001, 2020.https://doi.org/10.3390/s20072001

[8] F. Mishri, and R. Ali. "Detection and Classification of Brain Tumours from MRI Images Using VGG16 Deep Learning Algorithm." *Wadi Alshatti University Journal of Pure and Applied Sciences*, vol. 3, no. 1, pp. 43-50, 2025. https://waujpas.com/index.php/journal/article/view/107

[9] W. Van Eeden, et al. "Micro-Doppler radar classification of humans and animals in an operational environment." *Expert Systems with Applications*, vol. 102, pp. 1-11, 2018. https://doi.org/10.1016/j.eswa.2018.02.01

[10] R. Guendel, et al. "Multipath exploitation for human activity recognition using a radar network." *IEEE Transactions on Geoscience and Remote Sensing*, vol. 62, pp. 1-13, 2024. https://doi.org/10.1109/TGRS.2024.3363631

[11] T. Zugno, et al. "Implementation of a spatial channel model for ns-3." *Proceedings of the 2020 Workshop on ns-3*, 2020. https://doi.org/10.1145/3389400.3389401

[12] A. Hanif, M. Muaz, A. Hasan, and M. Adeel. "Micro-Doppler Based Target Recognition With Radars: A Review." *IEEE Sensors Journal*, vol. 22, pp. 2948-2961, 2022. https://doi.org/10.1109/JSEN.2022.3141213.

[13] M. Buyukakkaslar, M. Erturk, and M. Aydin. "A review on radar-based human detection techniques." *Sensors*, vol. 24, no. 17, p. 5709, 2024. https://doi.org/10.3390/s24175709

[14] Z. Wang, et al. "Recognition of approximate motions of human based on Micro-Doppler features." *IEEE Sensors Journal*, vol. 23, no. 11, pp. 12388-12397, 2023. https://doi.org/10.1109/JSEN.2023.3267820

[15] Q. Zhu, et al. "3GPP TR 38.901 channel model." *The Wiley 5G Ref: The Essential 5G Reference Online*, Wiley Press, pp. 1-35, 2021. https://www.researchgate.net/publication/348790466

[16] T. Sakamoto. "Personal identification using ultrawideband radar measurement of walking and sitting motions and a convolutional neural network." *arXiv preprint arXiv:2008.02182*, 2020. https://doi.org/10.1587/transinf.2018EDP7435

[17] J. Shi, et al. "Human activity recognition based on feature fusion of millimeter wave radar and inertial navigation." IEEE Journal of Microwaves, 2025. https://doi.org/10.1109/JMW.2025.3539957

[18] Z. Chen, Y. Sun, and L. Qu. "Research on cross-scene human activity recognition based on radar and wi-fi multimodal fusion." *Electronics*, vol. 14, no. 8, p. 1518, 2025. https://doi.org/10.3390/electronics14081518

[19] H. Cui, et al. "Milipoint: A point cloud dataset for mmwave radar." *Advances in Neural Information Processing Systems*, vol. 36, pp. 62713-62726, 2023. https://doi.org/10.48550/arXiv.2309.13425

[20] Y. Liu, et al. "Echoes beyond points: Unleashing the power of raw radar data in multi-modality fusion." *Advances in Neural Information Processing Systems*, vol. 36, pp. 53964-53982, 2023. https://doi.org/10.48550/arXiv.2307.16532

[21] B. Galkin, J. Kibilda, and L. DaSilva. "Coverage analysis for low-altitude UAV networks in urban environments." *GLOBECOM 2017-2017 IEEE Global Communications Conference*, IEEE, 2017. https://doi.org/10.1109/GLOCOM.2017.8254658

[22] A. Sesyuk, S. Ioannou, and M. Raspopoulos. "3d millimeter-wave sensing vs ultra-wideband positioning." *2024 14th International Conference on Indoor Positioning and Indoor Navigation (IPIN)*, IEEE, 2024. https://doi.org/10.1109/IPIN62893.2024.10786158

[23] T. Rappaport, et al. "Wireless communications and applications above 100 GHz: Opportunities and challenges for 6G and beyond." *IEEE Access*, vol. 7, pp. 78729-78757, 2019. https://doi.org/10.1109/ACCESS.2019.2921522

[24] B. Figueiredo, et al. "A Review: Radar Remote-Based Gait Identification Methods and Techniques." *Remote Sensing*, vol. 17, no. 7, p. 1282, 2025. https://doi.org/10.3390/rs17071282

[25] H. Yang, Y. Zhang, and W. Ding. "Multiple heterogeneous P-DCNNs ensemble with stacking algorithm: A novel recognition method of space target ISAR images under the condition of small sample set." *IEEE Access*, vol. 8, pp. 75543-75570, 2020. https://doi.org/10.1109/ACCESS.2020.2989162

[26] H. Rahman. "Fundamental principles of radar". CRC Press, 2019. https://www.scribd.com/presentation/826452223/NAV-5-Fundamental-Principles-of-Radar-20250122-231713-0000

[27] B. Ma, and B. Chen. "A 1D cascaded denoising and classification framework for Micro-Doppler-based radar target recognition." *Remote Sensing*, vol. 17, no. 9, p. 1515, 2025. Htps://doi.org/10.3390/rs17091515

[28] Y. Zhao, et al. "Human activity recognition based on non-contact radar data and improved PCA method." *Applied Sciences*, vol. 12, no. 14, p. 7124, 2022. https://doi.org/10.3390/app12147124

[29] S. Kumar, and P. Gupta. "Performance analysis of Rayleigh and Rician fading channel models using Matlab simulation." *International Journal of Intelligent Systems and Applications*, vol. 5, no. 9, pp. 94-102, 2013. https://www.researchgate.net/publication/251232606

[30] D. Buchman, et al. "Pedestrian and animal recognition using doppler radar signature and deep learning." *Sensors*, vol. 22, no. 9, p. 3456, 2022. https://doi.org/10.3390/s22093456

[31] A. Darlis, et al. "Autonomous human and animal classification using synthetic 2d tensor data based on dual-receiver mmwave radar system." IEEE Access, vol. 11, pp. 80284-80296, 2021.https://doi.org/10.1109/ACCESS.2023.3299325

[32] Blal, Zohra, Rasim Ali, and Salam Yasser. "Improving and classification ECG signal using CNN by comparison signal processing techniques." *Wadi Alshatti University Journal of Pure and Applied Sciences*, vol.2, no.2,pp. 99-103, 2024. https://waujpas.com/index.php/journal/article/view/88